The Role of Molecular Rayleigh Scattering in the Enhancement of Clear Sky Reflectance in the Vicinity of Cumulus Clouds

GUOYONG WEN, University of Maryland Baltimore County, Maryland

ALEXANDER MARSHAK, AND ROBERT F. CAHALAN, NASA/Goddard Space Flight Center

(Manuscript for Submission to *Journal of Geophysical Research)*

Revised June 10, 2008

Clouds increase the complexity of the radiative transfer process, particularly for aerosol retrievals in clear regions in the vicinity of clouds. This study focuses on identifying mechanisms responsible for the enhancement of reflectance in clear regions in the vicinity of cumulus clouds, and quantifying the relative importance of each mechanism. Using cloud optical properties and surface albedo derived from ASTER and MODIS, we performed extensive Monte Carlo simulations of radiative transfer in two cumulus scenes in a biomass burning region in Brazil. The results show that the interaction between clouds and molecular Rayleigh scattering above clouds is the dominant mechanism for the enhancement of visible reflectance in clear regions in boundary layer cumulus field over dark surfaces. The Rayleigh scattering contributes ~80% and ~50% to the total enhancement for the wavelengths 0.47μm and 0.66μm, respectively. Out of the total contribution of molecular scattering, ~90% arises from the atmosphere above clouds; there is little contribution to the enhancement from the atmosphere below clouds. The dominant mechanism responsible for the cloud-induced enhancement of clear sky reflectance in the vicinity of clouds provides theoretical basis and simplifications for future aerosol remote sensing from satellite.

1. INTRODUCTION

Aerosol and cloud are two important components of the Earth's atmosphere. Understanding the interaction between aerosols and clouds is particularly important in studying the direct and indirect effects of aerosols on climate and cloud processes. Satellite observations provide a unique opportunity to study aerosol and cloud interactions on a global scale. Previous efforts have been made to study the relationship between aerosol optical thickness and cloud properties [e.g., *Sekiguchi et al.*, 2003; *Loeb and Manalo-Smith*, 2005; *Zhang et al.*, 2005; *Ignatov et al.*, 2005; *Kaufman et al.*, 2005; *Kaufman and Koren*, 2006]. *Koren et al*. [2007] recently reported a "twilight" zone near cloud edges, and commented that "the total aerosol direct forcing may be significantly higher than is currently estimated due to large contributions from this transition zone."

Regions near cloud edges are important in studying aerosol and cloud interactions, and satellite observations are valuable to this research. However, using satellite observations to effectively study aerosol-cloud interaction remains a challenge. One of the problems is that reflected sunlight in clear regions in the vicinity of clouds is affected by nearby clouds. Studies have shown that clouds increase the reflectance of nearby clear regions, leading to large biases in aerosol optical thickness retrievals from satellite observations [e.g., *Cahalan et al.*, 2001; *Wen et al.*, 2001; *Nikolaeva et al.*, 2005; *Wen et al.*, 2006, 2007; *Yang and Di Girolamo*, 2008]. Recently, Kassianov and Ovchnnikov [2008] proposed a reflectance ratio method to retrieve aerosols in the presence of cumulus clouds.

Our previous studies focused on quantifying the magnitude of the enhancement and associated bias in aerosol retrievals. This study is an extension of our previous work [*Wen et al.,* 2006; 2007] with an emphasis on identifying the physical mechanisms responsible for the reflectance enhancement. We will show that molecular scattering above boundary layer clouds is the dominant mechanism to the cloud-induced visible reflectance enhancements in near by clear regions. The results apply to boundary layer clouds over dark surfaces. Those low clouds preferably occur in the subtropical eastern oceans, over the high-latitude oceans, where stratus regimes are best developed, and in regions of intense tropical convection, such as the Bay of Bengal during JJA and over the Amazon in Indonesia during DJF [see *Hartmann et al.*, 1992]. Since "the largest contributions to net cloud forcing are provided by low clouds, especially in the tropical stratus cloud regions and the summer hemisphere" [*Hartmann et al.*, 1992], results of this work are significant to understanding aerosol-cloud interactions.

In section 2, we briefly describe the aerosol and cloud properties used in the Monte Carlo simulation. Section 3 describes our method of analysis. The results are presented in section 4 and summarized and discussed in Section 5.

2. CLOUD FIELDS AND AEROSOL PROPERTIES

Two high-resolution images of cumulus cloud fields for two MODIS aerosol bands at 0.47μm and 0.66μm are used in this study. They are sub-images of an ASTER image collocated with a MODIS image acquired on January 25, 2003. The ASTER image is centered on the equator at 53.78° West with solar zenith angle (SZA) of 32° and solar azimuth angle of 129°. The same images were used by *Wen et al.* [2007] to study three dimensional (3D) cloud effects on the enhancement in clear regions of cumulus scenes. The two cloud fields are 15 km x 15 km in size. The cloud optical depth of both images is retrieved from ASTER observations at 90-m resolution using a lookup table similar to that for MODIS cloud retrieval [*Platnick et al.*, 2003]. The averaged cloud optical depths are 14 for the "thick" cloud and 7 for the "thin" cloud (Fig. 1). The cloud fractions are 59% and 51% for thick and thin cloud, respectively. The cloud base is assumed to be constant at 1 km. Cloud top heights are estimated from brightness temperature at 11μm (ASTER band 14) for both clouds. The average cloud top height is 1.5 km and 2 km for the thin clouds and thick clouds, respectively. The vertical profile of cloud liquid water is assumed to be linear. Single scattering properties of clouds, such as the phase function and single scattering albedo at the two MODIS bands, are computed assuming a gamma distribution of cloud droplets with an effective radius of 10μm and an effective variance of 0.1 [*e.g.*, *Hansen*, 1974].

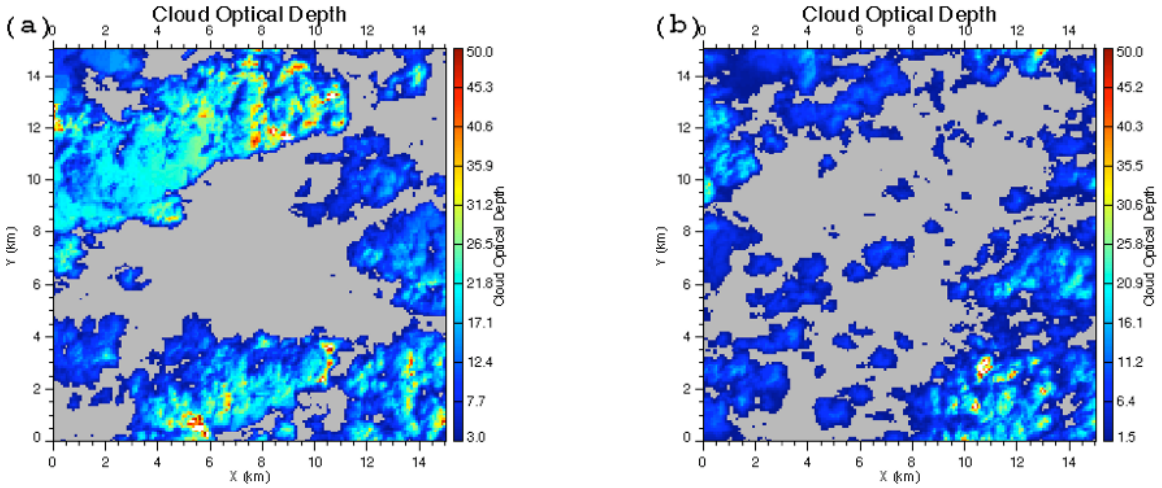

Figure 1. Cloud optical depth of (a) thick and (b) thin clouds. The average cloud optical depth is ~14 and ~7 with cloud cover of 59% and 51% for the thick and thin cloud respectively.

In biomass burning regions of Brazil, a strong trade wind inversion caps the shallow cumulus, and traps most aerosols in the atmospheric boundary layer [*Reid et al.*, 1998]. Here we assume that horizontally stratified aerosols are distributed in two distinctive vertical layers of the atmosphere: the boundary layer and the free troposphere. Most aerosols are trapped in the boundary layer, approximately 2 km thick. A small amount of aerosol, with optical thickness 0.01, is assumed in the free troposphere from 2 km to 10 km. We assume that aerosols are distributed uniformly in the vertical with a constant extinction in each layer. The model atmosphere is schematically shown in Fig. 2a with vertical distributions of aerosol and molecular scattering optical thickness at two MODIS aerosol bands and cloud base and average cloud top heights indicated (Fig. 2b). Aerosol particles are assumed to have a lognormal size distribution with modal radius of 0.13μm and a standard deviation of the natural logarithm of the radius of 0.6, and a single scattering albedo of 0.9, similar to the aerosol model in the MODIS aerosol algorithm [*Remer et al.*, 1998; 2005]. Aerosol phase functions are computed using Mie scattering theory. Aerosol phase function at 0.47μm is presented in Fig. 3 to compare with the phase function of Rayleigh scattering for discussions in latter sections.

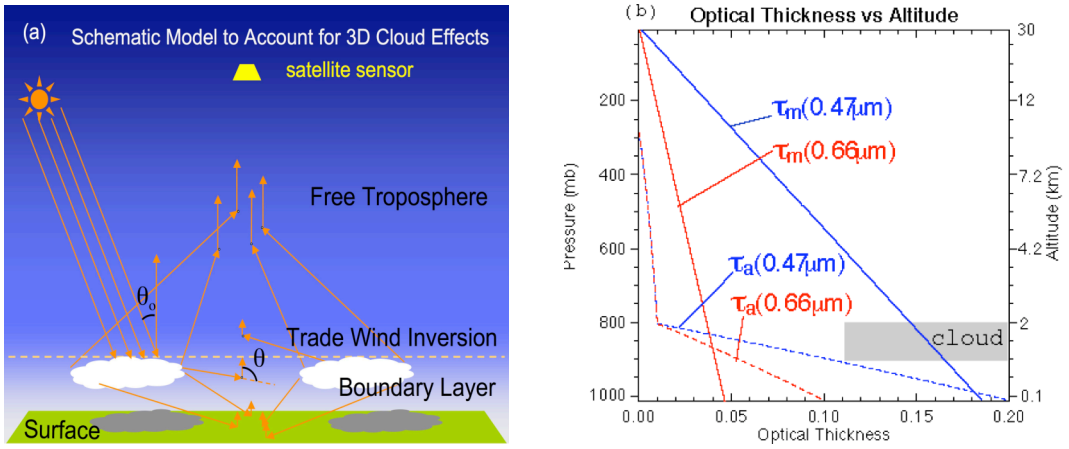

Figure 2. (a) Cumulus clouds and aerosols are trapped in the boundary layer due to the trade wind inversion similar to that in *Reid et al.* [1998]. Solar zenith angle θ_o and the scattering angle θ are indicated; (b) Vertical distributions of molecular Rayleigh scattering optical thickness (τ_m) and aerosol optical thickness (τ_a) with cloud position indicated. The total optical thicknesses are $\tau_m(0.47\mu m)$ = 0.185, $\tau_m(0.66\mu m)$ =0.046, and $\tau_a(0.47\mu m)$=0.2, $\tau_a(0.66\mu m)$=0.1. Above cloud top molecular scattering optical thickness ($\tau_m(0.47\mu m)$~0.15, $\tau_m(0.66\mu m)$~0.04) are much larger than aerosol optical thickness ($\tau_a(0.47\mu m)$~$\tau_a(0.66\mu m)$~0.01).

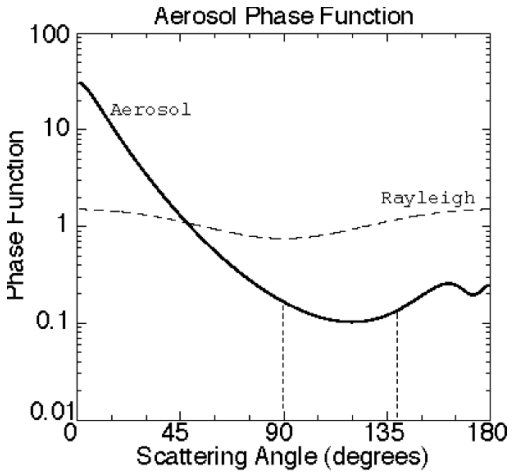

Figure 3. Aerosol phase function (solid) as compared with the molecular Rayleigh phase function (dashed) similar to those in Fig 6.3 in Thomas and Stamnes [1999]. Scattering angles below clouds (~90° to ~140°) are indicated.

The MODIS surface albedo product [*Moody et al.*, 2005] shows that the surface visible band reflectance is dark and homogeneous. So we use average surface albedos of 0.01 at 0.47μm and 0.02 at 0.66μm in this study.

Here we want to emphasize that cumulus clouds and most aerosols in the boundary layer with dark surfaces are characteristic features of cloud fields in this study. Those low clouds not only occur in regions of intense tropical convection in Amazon, they also preferably appear in the subtropical eastern oceans, over the high-latitude oceans [see *Hartmann et al.*, 1992]. Since "the largest contributions to net cloud forcing are provided by low clouds, especially in the tropical stratus cloud regions and the summer hemisphere" [*Hartmann et al.*, 1992], results of this work are significant to understanding aerosol-cloud interactions.

We use the atmospheric and surface optical properties as inputs to an Intercomparison of 3D Radiation Codes (I3RC) [*Cahalan et al.*, 2005] certified Monte Carlo (MC) code for radiative transfer in a 3D cloudy atmosphere [*Evans and Marshak*, 2005] to perform detailed studies on 3D effects on the reflectance enhancement in clear regions in cumulus cloud field, focusing on identifying major physical mechanisms for the reflectance enhancement.

3. METHOD

Sunlight reaching the planet Earth experiences scattering from molecules, aerosol particles, and surface reflection. Radiation received by an Earth-viewing satellite sensor is a sum of radiation scattered into the viewing direction from each layer of the atmosphere. To know the contribution from different layers of the atmosphere and from different scattering species is critical to understanding the radiative processes, remote sensing, and cloud effects on enhancing clear region reflectance.

3.1 CONTRIBUTION FUNCTIONS

The concept of contribution function was used by Dave and Mateer (1967) for studying the possibility of estimating total atmospheric ozone from satellite measurements. In their study, they examined contribution to the upward radiation for both primary scattering (single scattering) and all orders of scattering (multiple scattering). Though photons that contribute from an atmospheric layer to the upward radiation may originate from other layers due to multiple scattering, the contribution function does provide a measure of relative importance of each vertical layer in contributing to the upward radiation for a given atmospheric condition (see Fig.2 of Dave and Mateer, 1967). A concept similar to the contribution function is the weighting function for studying multiple scattering photon transport in cloud remote sensing introduced by Platnick [2000]. In present study the contribution function from different layers is extended to account for contributions from each individual scattering species, as described below.

To calculate the contribution from each species in each layer we use the local estimate method described in Evans and Marshak [2005]. The Monte Carlo scheme simulates photon trajectories, tracking where each scattering event occurs and what type of scattering species is involved using statistical methods. For given optical properties of the atmosphere this method computes contributions from each scattering species in each layer from each scattering event in the multiple scattering processes. In an atmosphere of N layers ($0 = z_0 < z_1 < \cdots < z_N = z_{TOA}$) with horizontal discrete grids (i.e., $x_1 < x_2 < x_3 \cdots; y_1 < y_2 < y_3 \cdots$), over a grid box (i,j) (i.e., $x_i \le x < x_{i+1},\ y_j \le y < y_{j+1}$), let's use $r_a(x,y,z_k), r_m(x,y,z_k)$ for the contribution from aerosols, molecules in layer k, and $r_s(x,y)$ for contribution from surface to the TOA reflectance $R(x,y)$, then

$$R(x,y) = \sum_{k=1}^{Nz} \left(r_a(x,y,z_k) + r_m(x,y,z_k) \right) + r_s(x,y) \quad (1)$$

where N_z is the number of atmospheric layers. For example, in a two-layer atmosphere with the total reflectance $R(x,y) = 0.15$, the partitions $r_a(x,y,z_1) = 0.01$, $r_m(x,y,z_1) = 0.02$, $r_a(x,y,z_2) = 0.02$, $r_m(x,y,z_2) = 0.08$, $r_s(x,y) = 0.02$ can be interpreted as for the total of 15% of reflected photons, on average 1% and 2% are contributed by aerosols and molecules in the first layer, and 2% and 8% are contributed by aerosols and molecules in the second layer, while 2% are from the surface reflection.

To illustrate the difference between single scattering and multiple scattering, we show examples for reflectance and associated partitions in clear atmospheric conditions. We performed a series of computation for solar zenith angle of 30° with molecular and aerosol properties described in section 2 and surface albedos of 0.1 and 0.2 for wavelengths 0.47μm and 0.66μm, respectively. The single scattering counts for a large portion (~72%) of reflected radiation at 0.47μm and an even larger fraction (~83%) of total reflectance at longer wavelength 0.66μm.

For wavelength 0.47μm, the partition of reflected radiation (surface, aerosol, molecule) is (0.066, 0.095, 0.839) for single scattering as compared to (0.065, 0.154, 0.781) for multiple scattering. For wavelength 0.66μm, the partition of reflected radiation for (surface, aerosol, molecule) is (0.397, 0.167, 0.436) for single scattering versus (0.370, 0.220, 0.410) for multiple scattering. From single scattering to multiple scattering, an increase of contribution about 5% from aerosols (for both wavelengths) and associated decrease of contribution from molecular scattering contribution (~6% for 0.47μm, ~3% for 0.66μm) are evident. The increase in aerosol contribution is because a large fraction of aerosols is in the lowest region of the atmosphere (see Fig. 2b) where multiple scattering occurs more. This is similar to what was found by Dave and Mateer [1967] (see their Fig. 2). A decrease of contribution from surface for both wavelengths is a result of blockage of surface reflected radiation by the atmosphere. Partitions of contributions from the Monte Carlo method capture additional contribution due to multiple scattering effects. Note that Kaufman et al., [1997] partitioned the path radiance into the one due to molecular scattering, and the one due to aerosol scattering using single scattering partition. Here we include multiple scattering in computing the contribution to TOA reflectance.

3.2 CONTRIBUTION TO THE ENHANCEMENT

To study cloud effects on reflectance in nearby clear regions we compute the effective contribution functions for 1D clear atmosphere and 3D atmosphere with clouds and examine the differences between them. First we define cumulative contribution functions. In an atmosphere of N layers ($0 = z_0 < z_1 < \cdots < z_N = z_{TOA}$), the cumulative contribution at an altitude z_M represents the contribution from the layers below z_M, and is defined as:

$$C_a(x,y,z_M) = \sum_{k=1}^{M} r_a(x,y,z_k) \quad (3.1)$$

$$C_m(x,y,z_M) = \sum_{k=1}^{M} r_m(x,y,z_k) \quad (3.2)$$

where $C_a(x,y,z)$ and $C_m(x,y,z)$ are cumulative contributions from aerosol and molecular scattering to the total outgoing radiance. For consistent notation $C_s(x,y)$ is used for the surface contribution in Eq (3.3).

$$C_s(x,y) = r_s(x,y) \qquad (3.3)$$

The TOA reflectances for 1D and 3D atmosphere are summations of contributions from each layer and from each type of scatterers as following.

$$R_{1D} = \sum_{k=1}^{N}\left(r_a(z_k) + r_m(z_k)\right) + r_s = C_{a,1D}(z_{TOA}) + C_{m,1D}(z_{TOA}) + C_{s,1D} \qquad (4.1)$$

and

$$R_{3D}(x,y) = \sum_{k=1}^{N}\left(r_a(x,y,z_k) + r_m(x,y,z_k)\right) + r_s(x,y) \qquad (4.2)$$
$$= C_{a,3D}(x,y,z_{TOA}) + C_{m,3D}(x,y,z_{TOA}) + C_{s,3D}(x,y)$$

Having cumulative contributions defined in Eqs (3.1)-(3.3), we further define the cumulative contribution to the enhancement (CCE) as the difference between the contribution in 3D atmosphere and its counterpart in 1D atmosphere, normalized by the total enhancement of the reflectance $\Delta R(x,y)$ at the top of the atmosphere (i.e., $\Delta R(x,y) = R_{3D}(x,y) - R_{1D}$) as follows:

$$\delta C_a(z) = \frac{\overline{C_{a,3D}(x,y,z)} - C_{a,1D}(z)}{\overline{\Delta R(x,y)}} \times 100 \qquad (5.1)$$

$$\delta C_m(z) = \frac{\overline{C_{m,3D}(x,y,z)} - C_{m,1D}(z)}{\overline{\Delta R(x,y)}} \times 100 \qquad (5.2)$$

$$\delta C_s = \frac{\overline{C_{s,3D}(x,y)} - C_{s,1D}}{\overline{\Delta R(x,y)}} \times 100 \qquad (5.3)$$

where overbars indicate the horizontal average. δC_s, $\delta C_a(z)$, and $\delta C_m(z)$ are percent contributions to the reflectance enhancement from surface, aerosol, and molecular Rayleigh scattering from layers below z. $\delta C(z_2) - \delta C(z_1)$ is the percent contribution from a layer between z_1 and z_2. All parameters and definitions are listed in Table I.

4. RESULTS

The CCE is useful to demonstrate the contribution from different scattering species as a function of altitude, as well as the surface contribution. By comparing relative contributions from scattering species in each layer and from surface, we will show that molecular scattering above clouds is the major physical mechanism responsible for the cloud-induced reflectance enhancement. We will further discuss the physics that leads to this conclusion. In section 4.1, we first examine CCE in clear regions in two cumulus cloud fields over dark surfaces and given aerosol optical thicknesses. In section 4.2, we examine the sensitivity of the CCE of molecular scattering and the total enhancement to the surface albedo and aerosol optical thickness.

4.1 VERTICAL DISTRIBUTION OF CONTRIBUTION TO THE ENHANCEMENT

It is worthwhile to briefly review some typical features of the enhancement of reflected radiation in clear regions in a cumulus cloud field. The enhancement of the clear region reflectance has large variability near cloud edges, with strong enhancement in the sunlit side and small enhancement (often negative) over cloud shadows. The enhancement becomes less variable at about 1 km away from cloud edges [see Fig. 12 in *Wen et al.*, 2007]. To avoid large variations, we focus on clear regions 1 km away from cloud edges in this study. The CCE presented in the following is horizontally averaged excluding cloud shadowed and illuminated areas, for thick and thin cloud scenes. To focus on the vertical distribution of the contribution, we assume the aerosol optical thickness is 0.2 at 0.47μm and 0.1 at 0.66μm (Fig. 2b). The surface albedo is 0.01 for 0.47μm and 0.02 for 0.66μm. Sections 4.1a and 4.1b present results for SZA=32° for thick and thin cloud scenes. Section 4.1c shows results for a lower solar elevation, namely SZA=60°.

4.1a CONTRIBUTIONS IN THICK CLOUDS

Figs. 4a, 4b show CCE (Eqs. 5.1-5.3) for clear regions in the thick cloud scene (Fig. 1a) at wavelengths of 0.47μm and 0.66μm, respectively. The surface contribution and vertical distributions of CCE for aerosol, molecular scattering, together with the summation of three components are plotted separately for both wavelengths. The relative contribution from surface, which is independent of altitude, is plotted as a straight vertical line. The pressure in vertical axis is proportional to molecular scattering optical thickness as shown in Fig. 2b.

For 0.47μm (Fig. 4a), the surface contribution is very small ($\delta C_s \sim 2\%$). Aerosols contribute $\delta C_a(z_{TOA}) \sim 15\%$ and molecular Rayleigh scattering contributes $\delta C_m(z_{TOA}) \sim 83\%$ to the total reflectance enhancement ~0.019 at the TOA. Out of the total molecular contributions, about 90% (i.e., $\delta C_m(z_{TOA}) - \delta C_m(z_{cloud\ top})$) is from the atmosphere above cloud top.

For 0.66μm (Fig. 4b), the surface is slightly brighter than that for 0.47μm, but its relative contribution is much higher. The surface, aerosol, and molecular Rayleigh scattering contribute $\delta C_s \sim 16\%$, $\delta C_a(z_{TOA}) \sim 28\%$ and $\delta C_m(z_{TOA}) \sim 56\%$, respectively, to the total reflectance enhancement of ~0.008 at the TOA. Again we see that out of the total contribution of molecular Rayleigh scattering, about 90% is from atmosphere above cloud top.

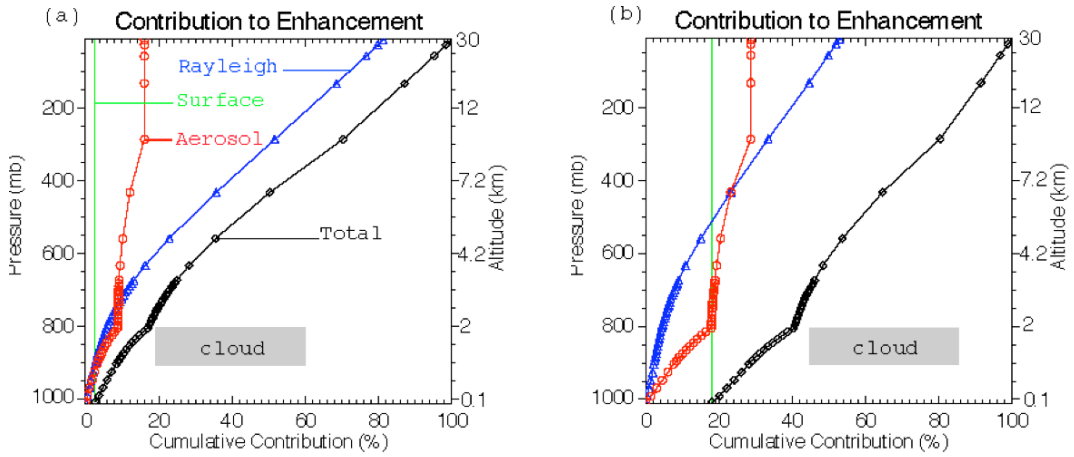

Figure 4. The CCEs for clear regions (1 km away from clouds) in the **thick** cumulus fields (Fig. 1a) for SZA= 32° with cloud position indicated: (a) for wavelength at 0.47μm; and (b) for wavelength 0.66μm. Lines with circles are for CCE from aerosol scattering; lines with triangles are for CCE from Rayleigh scattering; straight lines are for CCE from surface contribution; lines with diamonds are the sums of all contributions to the enhancement. Molecular Rayleigh scattering contributes 82% and 52% to the TOA reflectance enhancements at 0.47μm and 0.66μm, respectively. The total reflectance enhancement due to clouds is 0.019 for 0.47μm and 0.008 for 0.66μm.

The CCEs have distinctive features in two regions of the atmosphere: above and below clouds (Figs. 4a, 4b). For molecules, the increase of CCE is much faster in the layer above clouds as compared to the layer below clouds. The contribution from atmosphere above cloud is about 90% of total molecular scattering contribution. Aerosol contribution is mainly from the layer below clouds where most aerosols are. Although, aerosol optical thickness is significantly larger than molecular scattering optical thickness in the boundary layer, aerosols contribute a small fraction to the reflectance enhancement. In the following we discuss the physics for the contributions from the two layers.

The single scattering approximation is often used to illustrate physical processes in aerosol studies [*e.g.*, *Kaufman et al.*, 1997; *Tanre et al.*, 1997; *Moulin et al.*, 1997; *Remer et al.*, 2005]. Using the single scattering approximation one can easily show that the contribution from a clear atmosphere to the enhancement of the TOA reflectance, Δr, is proportional to the cloud diffuse radiation, F_{diff}, scattering optical depth of aerosols and molecules $\boldsymbol{\tau}$, and associated scattering phase function $P(\boldsymbol{\theta})$ at the scattering angle $\boldsymbol{\theta}$ [*e.g.*, *Hansen*, 1974]

$$\Delta r \sim F_{diff} \cdot \boldsymbol{\tau} \cdot P(\boldsymbol{\theta}) \qquad (6)$$

Thus cloud diffuse radiation, scattering optical thickness of aerosols and molecules, and associated phase function are the three major factors that determine contributions from each layer to the atmosphere TOA reflectance enhancement.

Before making further discussions, we want to show that the cloud diffuse radiation below clouds is significantly smaller than that above clouds. To illustrate this point we compute CCE for molecular atmosphere with no aerosols and surface reflection (Fig. 5). The CCE is a linear function pressure or molecular scattering optical thickness above and below clouds. (Note molecular scattering optical thickness is proportional to the pressure.) However, the rate of increase of the CCE below cloud is much smaller than above cloud. Since molecular scattering phase function depends weakly on scattering angle, a slower rate of increase of the CCE below clouds implies a smaller cloud diffuse radiation compared to the region above clouds. One can further estimate the relative strength of diffuse radiation below and above clouds. Assuming a constant phase function in From Eq. (6) one can derive

$$F_{diff}(below) \sim \frac{\Delta r(below)}{\Delta r(above)} \frac{\boldsymbol{\tau}(above)}{\boldsymbol{\tau}(below)} \cdot F_{diff}(above) \qquad (7)$$

where "below" and "above" indicate layers below and above cloud top, respectively. Using relative contributions and molecular optical thicknesses of the two layers ($\Delta r(below) \sim 8\%$, $\Delta r(above) \sim 92\%$; $\boldsymbol{\tau}(below) \sim 0.037$, $\boldsymbol{\tau}(above) \sim 0.148$ at 0.47μm), one can see that the average diffuse radiation below cloud is about 1/3 of that above the cloud.

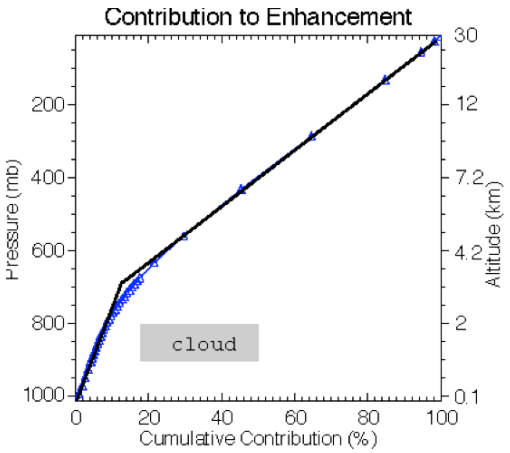

Figure 5. Same as the CCE in Fig. 4 but for molecular atmosphere with no aerosols and surface reflection for wavelength at 0.47µm (line with diamonds). Two straight lines schematically show the two vertical distinctive layers in clear areas near clouds. The total reflectance enhancement due to clouds is ~0.018.

Boundary layer clouds are very reflective and provide diffuse radiation above cloud. Above clouds molecules are the primary scatterers. For boundary layer clouds with cloud top about ~2 km (or ~800mb), molecular Rayleigh scattering optical thickness is about 80% of the total molecular optical thickness. Molecular optical thicknesses above clouds (~0.15 at 0.47µm and ~0.04 at 0.66µm) are considerably larger than the aerosol optical thickness of 0.01 (for both wavelengths) in the free troposphere (Fig. 2b). Strong wavelength dependence of molecular scattering optical thickness and almost wavelength neutral visible cloud albedo lead to a larger enhancement for the blue band than the red band. One should note that the aerosol scattering phase function has a strong forward peak resulting in a larger increase of CCE from aerosols in higher altitudes.

Below clouds, the radiative interactions between clouds and scatterers in clear areas occur when photons transmitted through cloud base or scattered from cloud sides collide with aerosols or molecules. This interaction contributes only a small fraction to the TOA reflectance due to the following factors: (1) the cloud diffuse radiation is small, only about 1/3 of that above clouds; (2) molecular scattering optical thickness is small, i.e., ~0.04 at 0.47µm and ~0.01 at 0.66µm (Fig. 2b); (3) aerosol phase function reaches minimum values of about one order of magnitude smaller than that for Rayleigh scattering (Fig. 3). Though aerosol scattering optical thickness is much larger compared to that for molecules, aerosols in this layer do not make large contributions to the TOA enhancement of clear sky reflectance.

For a dark surface, the contribution to the enhancement is small. Although surface is dark for both bands, the surface albedo at the red band is twice as large as that for the blue band. Since molecular Rayleigh scattering is weaker for longer wavelengths and contributes less to the total enhancement, the percentage contribution from surface is expected to be larger for the red band as compared to the blue band.

It becomes evident now that cloud-molecule radiative interaction above cloud is the major physical mechanism for the cloud-induced reflectance enhancement in clear regions near boundary layer cumulus clouds over dark surfaces. And this has been explained by associated scattering optical thickness, scattering phase function, and cloud diffuse radiation below and above clouds.

4.1b CONTRIBUTIONS IN THIN CLOUDS

The enhancement at the TOA is smaller in the thin cloud scene (Fig. 1b) as compared to that in the thick cloud scene (Fig. 1a) for both wavelengths. At 0.47µm the cloud-induced enhancement in clear regions of thin cloud scene is ~0.012 as compared to ~0.019 in the thick cloud scene; and at 0.66µm the enhancement is ~0.005 for the thin cloud scene compared to ~0.008 in the thick cloud scene. However, CCEs for thin cloud scene are similar to those for thick clouds. Here we show the increase of CCEs in the thin cloud fields as compared to those in the thick cloud field in Fig. 6. At 0.47µm, there is little change in molecular Rayleigh scattering contributes below 500 mb (or ~5km) with a decrease up to ~4% to molecular contributions at the TOA. Percent contribution from aerosols increases with height in the boundary layer up to ~3%, and does not change in the free troposphere. Surface contribution increases by 1.5%. For the longer wavelength 0.66µm, a slightly larger decrease in the contribution from molecular Rayleigh scattering (~7%) is associated with a little increase in the contribution from surface reflection (~6%) as compared to the wavelength 0.47µm. It is interesting to note that the percent contribution from aerosol has little change though out the atmosphere.

Though the contribution from molecular Rayleigh scattering is a little less as compared to that in the thick cloud fields, it is still the major mechanism to the reflectance enhancements in clear regions in the thin cloud fields.

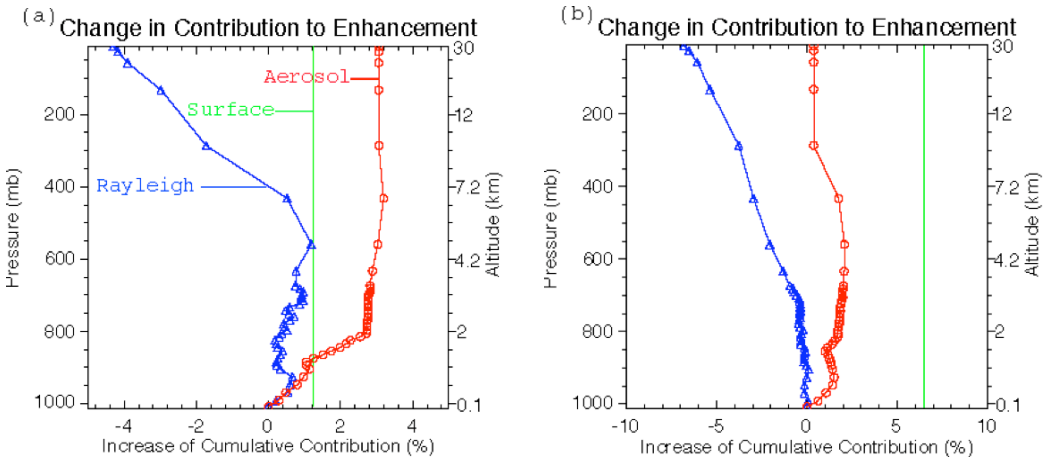

Figure 6. CCEs for clear regions in the **thin** cumulus cloud fields (Fig. 1b) are similar to those in the **thick** cumulus cloud fields (Fig. 1a). Increase of CCEs compared to those in the **thick** cumulus cloud fields is plotted (a) for wavelength at 0.47μm; and (b) for wavelength 0.66μm. In the **thin** cloud fields, the contribution from molecular scattering decreases by 4-7%; contributions from surface reflection decrease by ~1.5% for 0.47μm and ~6% for 0.66μm; contributions from aerosol scattering increase by ~3% for 0.47μm. The total reflectance enhancement due to clouds is ~0.012 for 0.47μm and ~0.005 and 0.66μm (SZA= 32°).

4.1c CONTRIBUTIONS FOR LOW SOLAR ELEVATION

Sections 4.1a and 4.1b examine contributions to the enhancement of clear region reflectance in the vicinity of clouds for a specific SZA of 32° when images were acquired. It is useful to examine the contributions for a lower solar elevation for the interests of understanding the radiative processes for alternative situations. Here we demonstrate the results for a SZA of 60° to examine the solar angle dependence of the enhancement.

A lower sun casts longer cloud shadow. For a cloud with a base height of 1km, cloud shadows is ~1.73km long from cloud edges for SZA of 60° (cloud height times tan(SZA)). For thick cloud scene the enhancement reaches the "asymptotic values" (see Wen *et al.*, 2006) at a distance about 1.8km away from cloud edges for thick clouds. For the thin clouds, clear areas are not as large as those in the thick clouds (see Fig. 1b). Only a few pixels are not affected by either sunlit side illumination effect or shadowing effect. Therefore, we only consider the thick cloud scene (Fig. 1a) for low solar elevation study.

In clear regions in the thick cloud scene (Fig. 1a), the total enhancement for low solar elevation is slightly larger than that for high solar elevation for the two wavelengths. From the high sun (SZA=32°) to the low sun (SZA=60°), the total reflectance enhancement increases by ~0.001 for both wavelengths, or ~5% and ~12% for 0.47μm, and 0.66μm, respectively.

CCEs in clear regions of the thick cumulus scene for SZA of 60° for the same aerosol, cloud, and surface properties (Fig. 7) are similar to those for the high solar elevation (Fig. 4). The same physical mechanisms for high solar elevation apply to interpret the vertical distribution of contributions. One can see that molecular Rayleigh scattering contributes $\delta C_m(z_{TOA}) \sim 89\%$ for 0.47μm and $\delta C_m(z_{TOA}) \sim 62\%$ for 0.66μm to the TOA enhancement. More than 90% of molecular Rayleigh scattering contributions are from atmosphere above cloud.

From the high sun to the low sun, an increase of ~6% in relative contribution from molecular Rayleigh scattering is evident. This increase is associated with decreases of relative contribution from surface reflection (~1-2%) and aerosol scattering (~4-5%).

Further computations are performed for a large range of solar zenith angles. For SZA from 0° to 60°, we found that the enhancement increases by ~10% and ~20% for 0.47μm and 0.66μm, respectively. Here we reiterate that shadowed pixels and pixels near the illuminated side of cloud edges are excluded because the reflectance of those pixels is so variable [*Wen et al.*, 2007]. In fact the MODIS aerosol algorithm effectively avoid those pixels by excluding fractions of darkest and brightest pixels [*Remer et al.*, 2005].

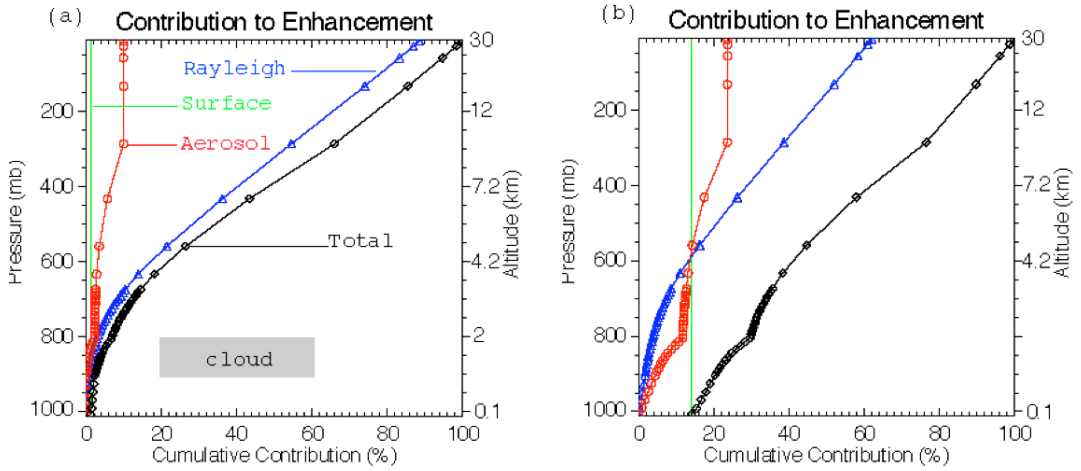

Figure 7. Similar to Figure 4 but for solar zenith angle of 60°. The CCE for clear regions (1.8 km away from clouds) in the **thick** cumulus fields (Fig. 1a): (a) for wavelength at 0.47μm; and (b) for wavelength 0.66μm. Molecular Rayleigh scattering contributes ~90% and ~62% to the TOA reflectance enhancements at 0.47μm and 0.66μm, respectively. The total reflectance enhancements are 0.02 for 0.47μm and 0.009 for 0.66μm.

For the same cloud fields, increase solar zenith angle leads to an increase of molecular scattering contribution, and a decrease of contribution from aerosols and surface reflection. Again molecular Rayleigh scattering from cloud top remains the dominant mechanism for low solar elevation.

4.2 DEPENDENCES ON SURFACE ALBEDO AND AEROSOL OPTICAL THICKNESS

The results in section 4.1 are for specified aerosol optical thickness and surface albedo. Here we examine the dependence of the enhancement on aerosol optical thickness and surface albedo. In this section we will show that the reflectance enhancement in clear areas in cumulus cloud fields over dark surfaces does not strongly depend on aerosol loadings, and molecular scattering above clouds is the major mechanism for the enhancement.

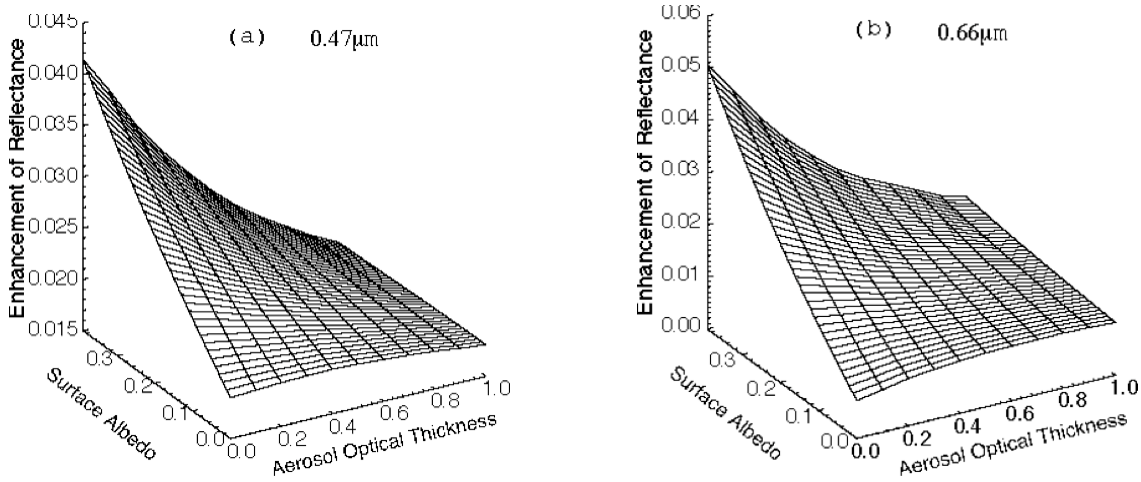

Figure 8. The total reflectance enhanceme ($\Delta R = R_{3D} - R_{1D}$) in thick cumulus scene as a function of aerosol optical thickness and surface albedo (a) for 0.47μm; and (b) for 0.66μm

Figure 8 shows the distribution of the total enhancement in thick cloud scene as a function of aerosol loading and surface albedo for the two wavelengths. For bright surfaces, the

enhancement decreases with aerosol optical thickness. This is because the surface contribution dominates the enhancement when surface is bright. As aerosol optical thickness increases, radiation from surface gets attenuated exponentially leading to a decrease in the enhancement. For dark surfaces, the enhancement depends weakly on aerosol loading particularly for wavelength 0.47μm. For a given aerosol optical thickness, the enhancement depends on the surface albedo, and such dependence is stronger at the longer wavelength. It is interesting to note that enhancement becomes less dependent on the surface albedo as aerosol loading increases, particularly for the shorter wavelength. It is also interesting to see that the enhancement at 0.66μm is larger than that at 0.47μm when aerosol loading is small (e.g., aerosol optical thickness is 0.01) and the surface is bright (e.g., surface albedo is 0.4). This is due to a much less atmospheric attenuation at the red band compared to the blue band.

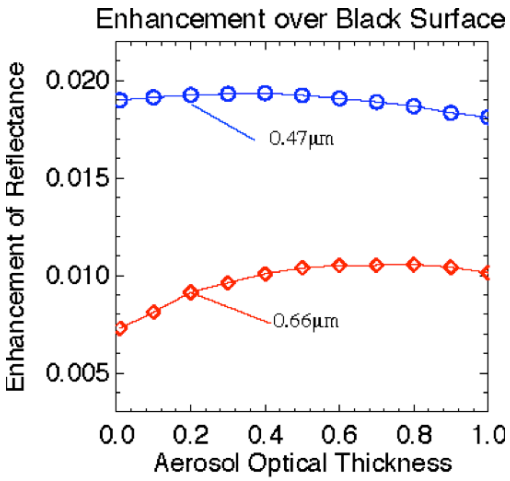

Figure 9. The total reflectance enhancement ($\Delta R = R_{3D} - R_{1D}$) over black surface in Fig. 7 (circle-line for 0.47μm; diamond-line for 0.66μm).

Zooming in Fig. 8 we examine the dependence of the cloud-induced enhancement on aerosol optical thickness for black surface in more detail in Fig. 9. For the blue band at 0.47μm, the cloud-induced enhancement increases slightly, reaching a maximum at aerosol optical thickness of ~0.4, then decreases gradually. Within a range of aerosol optical thickness from 0.01 to 1, the cloud-induced enhancement weakly depends on aerosol optical thickness. Similarly, the cloud-induced enhancement for the red band at 0.66μm also weakly depends on aerosol loading for aerosol optical thickness greater than 0.2. For wavelength 0.66μm, though the relative change of the enhancement is large (~40%) for an increase of aerosol optical thickness from 0.01 to 0.2, the absolute change is about 0.002 corresponding to an overestimate of 0.02 in aerosol optical thickness.

An increase of aerosol optical thickness has two competing effects to the enhancement. First, an increase of aerosol optical thickness will result a larger scattering optical thickness leading to an increase in the enhancement. When aerosol optical thickness continues to increase, the contrast between clouds and clear regions decrease. The smaller the contrast, the smaller the horizontal fluxes going from thicker to thinner areas leading to a decrease in the enhancement as discussed by *Marshak and Davis* [2005]. Nevertheless, it is evident that the magnitude of changes in the enhancement is small for a large range of aerosol optical thickness for both wavelengths.

It is interesting to examine the fractional contribution from molecular Rayleigh scattering, i.e. $\frac{\delta C_m(z_{TOA})}{\delta C_a(z_{TOA}) + \delta C_m(z_{TOA}) + \delta C_s}$. Fig. 10 shows the distribution of the fractional enhancement from molecular Rayleigh scattering to the total enhancement in Fig. 8. It is evident that the fractional contribution from molecular Rayleigh scattering depends on surface albedo, aerosol amount, and wavelength. The brighter the surface, the more relative contribution is from surface, and the less is the fractional contribution from molecular Rayleigh scattering. For bright surfaces the fractional contribution from molecular Rayleigh scattering increases with aerosol optical thickness. This is because aerosols block radiation from surface leading to a relative increase from molecular Rayleigh scattering. Over dark surface, molecular Rayleigh scattering contributes to a large portion of the enhancement, ~80% for 0.47μm and ~50% for 0.66μm.

After examining the total enhancement and the fractional contribution from molecular Rayleigh scattering for large range of surface albedo and aerosol loading, we conclude that the cloud-induced enhancement depends weakly on aerosol optical thickness over dark surfaces and molecular Rayleigh scattering is the major mechanism for the reflectance enhancement.

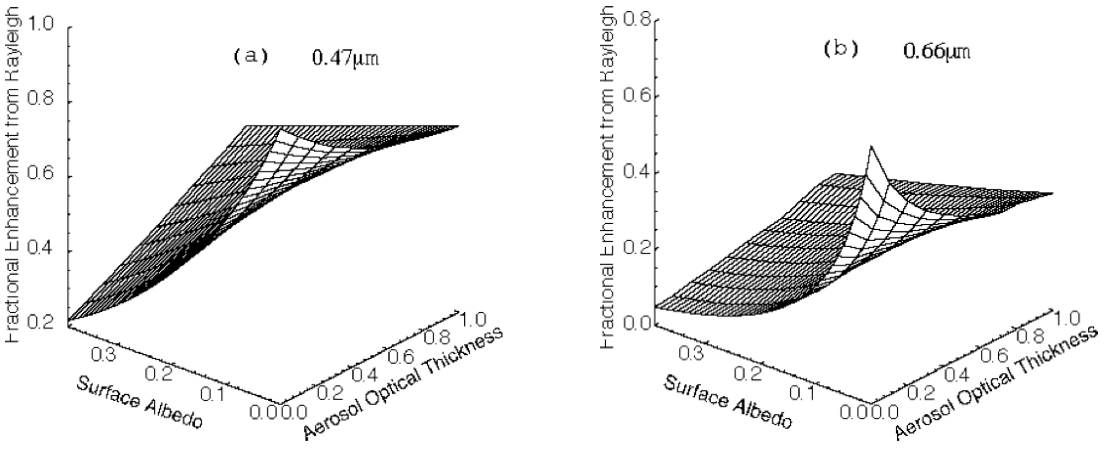

Figure 10. The distribution of the fractional enhancement from molecular Rayleigh scattering (i.e., $\frac{\delta C_m(z_{TOA})}{\delta C_a(z_{TOA}) + \delta C_m(z_{TOA}) + \delta C_s}$) in thick cumulus scene as a function of aerosol optical thickness and surface albedo (a) at 0.47μm; and (b) at 0.66μm. Molecular Rayleigh scattering contributes ~80% and ~50% for wavelength 0.47μm and 0.66μm when surface is dark. A strong dependence of fractional enhancement from molecular Rayleigh scattering on surface albedo is evident for small aerosol loadings.

5. SUMMARY AND DISCUSSIONS

This paper employs a Monte Carlo scheme to examine physical mechanisms of cloud 3D radiative effects on reflectances in nearby clear regions for two ASTER images collocated with a MODIS scene in a biomass burning region of Brazil. We found that molecular Rayleigh scattering above clouds is the dominant mechanism for cloud-induced enhancement of visible reflectances in clear regions over dark surfaces. This result applies to thin and thick cloud scenes, and for high and low solar elevations. This finding provides couple of simplifications for correcting cloud adjacency effects for remote sensing of aerosols in the vicinity of clouds, an important region for the understanding of cloud-aerosol interactions. Those simplifications include (1) details of aerosol loading and optical properties can be neglected in computing cloud adjacency effects; (2) neglecting aerosol amount below clouds and accounting only cloud-Rayleigh radiative interaction may provide a good approximation for correcting 3D cloud adjacency effects particularly for shorter wavelengths. The results apply to boundary layer clouds over dark surfaces. Those clouds preferably occur in the subtropical eastern oceans, over the high-latitude oceans, and in regions of intense tropical convection, such as the Bay of Bengal during JJA and over the Amazon in Indonesia during DJF [see *Hartmann et al.*, 1992]. Since "the largest contributions to net cloud forcing are provided by low clouds, especially in the tropical stratus cloud regions and the summer hemisphere" [*Hartmann et al.*, 1992], results of this work are significant to understanding aerosol-cloud interactions.

We found that the Rayleigh scattering contributes ~80% and ~50% to the total enhancement of visible reflectances in clear regions of cumulus clouds over dark surfaces for the wavelengths 0.47μm and 0.66μm, respectively. Out of the total contribution of molecular scattering, ~90% arises from the atmosphere above clouds. There is little contribution to the enhancement from the atmosphere below clouds. The percentage contribution from the dark surface is very small at 0.47μm, but relatively large at 0.66μm.

Recently, Kassianov and Ovtchinnikov [2008] proposed a technique for retrieving aerosol optical thickness in the presence of cumulus clouds assuming that $\Delta R_{3D}(\lambda) \approx \gamma R_{1D}(\lambda)$, where wavelength-independent parameter γ is a function of cloud properties. This assumption leads to $\frac{\Delta R_{3D}(\lambda_1)}{\Delta R_{3D}(\lambda_2)} \approx \frac{R_{3D}(\lambda_1)}{R_{3D}(\lambda_2)} \approx \frac{R_{1D}(\lambda_1)}{R_{1D}(\lambda_2)}$, where λ_1=0.66μm and λ_2=0.47μm in the present study. It is useful to validate this assumption with reflectances computed in the present study. For SZA=32° aerosol optical thickness of $\tau_a(\lambda_1)$=0.1, $\tau_a(\lambda_2)$ =0.2, and surface albedo of $\alpha_s(\lambda_2)$=0.01 and $\alpha_s(\lambda_1)$=0.02, from the 1D reflectances ($R_{1D}(\lambda_1)$=0.0427 and $R_{1D}(\lambda_2)$=0.0883) the ratio $\frac{R_{1D}(\lambda_1)}{R_{1D}(\lambda_2)} = 0.484$. Using the 3D reflectances ($R_{3D}(\lambda_1)$=0.0513 and $R_{3D}(\lambda_2)$=0.1081 in the thick cloud fields; $R_{3D}(\lambda_1)$=0.0483 and $R_{3D}(\lambda_2)$=0.0996 in the thin cloud fields), one find that the relative difference of the ratios of reflectances and

enhancements is about 2% and -10% for the thin and thick cloud fields, respectively.

Since molecular scattering cross sections have strong wavelength dependence for solar wavelengths, and cloud albedo is almost wavelength neutral in visible bands, the cloud-induced enhancement of reflectances in clear regions of cloud scenes decreases with wavelength. For the same atmospheric conditions the reflected solar radiation in clear regions near clouds is more bluish compared to that in regions far away from clouds.

We compared results for the thin cloud scene with those for the thick cloud scene. We found that a thicker cloud induces a larger enhancement compared to a thinner cloud. The magnitude of the increase of the enhancement due to the increase of cloud optical depth is wavelength dependent. For the same atmospheric conditions over dark surfaces, a thicker cloud is more effective to enhance the TOA clear sky reflectance at blue than at red wavelengths. From the thin cloud scene to the thick cloud scene, an increase in the relative contribution from molecular scattering is associated with a decrease in relative contributions from aerosols and surface. Nevertheless, molecular scattering above clouds is the dominant mechanism for the reflectance enhancement in clear areas near boundary layer clouds.

We also examined the SZA dependence of the enhancement. We found that an increase of SZA from 0° to 60° leads to increases about 10-20% in total enhancement. From high solar elevation to low elevation, an increase in the relative contribution from molecular scattering is associated with an increase of cloud albedo and a decrease in relative contributions from aerosols and surface. Molecular scattering above clouds as the dominant mechanism for the reflectance enhancements applies to both low and high solar angles.

We have performed extensive computations for a large range of aerosol optical thicknesses and variations of surface albedo. Our analyses demonstrate that for a given aerosol optical thickness the enhancement in clear regions of cumulus increases with surface albedo. However, the enhancement weakly depends on aerosol loading when the surface is dark.

Although results presented in this paper are for biomass burning aerosols that have single scattering albedo of ~0.9 [*Remer et al.*, 2005], we have also performed identical studies for non-absorbing aerosols that have single scattering albedo of 1. We found that the results are similar for both absorbing and non-absorbing aerosols. The enhancement is slightly larger (<5%) for the non-absorbing aerosols as compared to absorbing aerosols over dark surfaces. This is because the enhancement weakly depends on amount, and the molecular Rayleigh scattering is the dominant mechanism for the enhancement over dark surfaces.

We found that the enhancement strongly depends on aerosol amount above cloud. This is primarily due to the large increase of aerosol scattering phase function in the forward direction and available cloud diffuse radiation above clouds.

Results of this research apply to clear regions in the vicinity of boundary layer clouds over dark surfaces. With high albedo compared to the dark surface background, boundary layer clouds are expected to be most susceptible to changes in aerosol [*Platnick and Twomey*, 1994]. Simultaneous observations of cloud and nearby aerosol properties are essential for the understanding of aerosol indirect effects on climate from satellite. Our previous studies show that clouds enhance the reflectance in clear region near cloud edges leading to large biases in 1D operational aerosol retrievals [*Wen et al.*, 2006, 2007]. This research identifies that molecular scattering above boundary layer clouds is the dominant mechanism for cloud-induced reflectance enhancement in clear regions near cloud edges. Now the complicated problem of aerosol-cloud radiative interactions can be simplified using a two-layer model to quantify the cloud-induced enhancement in clear regions of a cloudy atmosphere [*Marshak et al.*, 2008].

However, this dominant physical mechanism is valid for boundary layer clouds above dark surface with a clean free troposphere above cloud top in visible wavelengths. Results of this study do not apply to all atmospheric conditions. Layers of dust aerosol at altitude above 3km were observed [e.g., *Kobayashi et al.*, 2003]. Smoke plumes can reach an altitude of 6 km [e.g., *Hoff*, 2005]. In such conditions, 3D cloud radiative effects are much more complex. Cirrus cloud at high altitude could potentially generate diffuse radiation to enhance the downward flux. Our results do not apply to convective clouds with large vertical extension. In near infrared wavelengths, the molecular scattering optical thickness is much smaller than that in visible wavelengths. Molecular Rayleigh scattering above cloud is no longer the dominant physical mechanism for near infrared spectrum of solar radiation. All these situations are potentially important in satellite remote sensing of aerosols, and require further research.

Table I. Definitions of symbols in the text.

Symbol	Definition
SZA	Solar zenith angle
z_k	The altitude of top of the *k*'th layer
R_{1D}	Reflectance of 1D clear atmosphere
$R_{3D}(x,y)$	Reflectance of 3D atmosphere
ΔR	Reflectance enhancement
$r_a(x,y,z_k)$	Contribution from aerosols to the reflectance from *k*'th layer
$r_m(x,y,z_k)$	Contribution from molecules to the reflectance from *k*'th layer
$r_s(x,y)$	Contribution from surface to the reflectance
$C_{a,1D}(z_M)$	Cumulative contribution to the reflectance from aerosols from layers below z_M for 1D
$C_{m,1D}(z_M)$	Cumulative contribution to the reflectance from molecules from layers below z_M for 1D
$C_{s,1D}$	Contribution to the reflectance from surface for 1D
$C_{s,3D}(x,y)$	Cumulative contribution to the reflectance from aerosols from layers below z_M for 3D
$C_{s,3D}(x,y)$	Cumulative contribution to the reflectance from molecules from layers below z_M for 3D
$C_{s,3D}(x,y)$	Contribution to the reflectance from surface for 3D
CCE	Cumulative contribution to the enhancement
$\delta C_a(z)$	CCE from aerosols from layers below z
$\delta C_m(z)$	CCE from molecules from layers below z
δC_s	Contribution to the enhancement from surface
F_{diff}	Cloud diffuse radiation
$P(\theta)$	Phase function at scattering angle θ
τ	Scattering optical thickness

Acknowledgments. This research was supported by funding provided by NASA and DoE's ARM program. We thank J. Coakley, N. Loeb, and L. Remer for useful discussions. The authors were greatly inspired by our colleague Yoram J. Kaufman in aerosol research.

REFERENCES

Andreae, M. O., D. Rosenfeld, P. Artaxo, A.A. Costa, G.P. Frank, K.M Longo, M.A.F. Silva-Dias (2004), Smoking Rain Clouds over the Amazon, *Science* , 303: 1337-1342 , DOI: 10.1126/science.1092779.

Cahalan, R. F., L. Oreopoulos, G. Wen, A. Marshak, S. C. Tsay, and T. P. DeFelice (2001), Cloud characterization and clear sky correction from Landsat 7. *Remote Sens. Environ.*, **78**, 83-98.

Cahalan, R.F., and coauthors (2005), The International Intercomparison of 3D Radiation Codes (I3RC): Bringing together the most advanced radiative transfer tools for cloudy atmospheres. *Bull. Amer. Meteor. Soc.*, **86** (9), 1275-1293.

Coakley, J. A., Jr., R. L. Bernstein, and P. A. Durkee (1987), Effect of ship-track effluents on cloud reflectivity, *Science*, 237, 1020-1022.

Dave, J.V., and C. L. Mateer (1967), A Preliminary Study on the Possibility of Estimating Total Atmospheric Ozone from Satellite Measurements, *J. Atmos., Sci.*, **24**, 414-427.

Davis, A.B., and Y. Knyazikhin (2005), A Primer in 3D Radiative Rransfer. In: Marshak, A., and A.B. Davis, [Eds], "*Three-Dimensional Radiative Transfer in Cloudy Atmospheres*", Springer, pp. 153-242.

Evans K. F. and A. Marshak (2005), Numerical Methods in Three-Dimensional Radiative Transfer. In: Marshak, A., and A.B. Davis, [Eds], "*Three-Dimensional Radiative Transfer in Cloudy Atmospheres*", Springer, pp. 243-282.

Feingold, G. (2003), Modeling of the first indirect effects: Analysis of measurement

requirements, *Geophy. Res. Lett.*, *30*(19), 1997, doi:10.1029/2003GL017967.

Feingold, G., R. Furrer, P. Pilewskie, L. A. Remer, Q. Min, and H. Jonsson (2006), Aerosol indirect effect studies at Southern Great Plains during the May 2003 Intensive Operations Period, *J. Geophy. Res.*, *111*, D05S14, doi:10.1029/2004JD005648.

Han, Q., W. Rossow, and A. Lacis (1994), Near-global survey of effective droplet radii in liquid water cloud using ISCCP data, *Journal of Climate*, 7, 465-497.

Hansen, J. (1974), Light scattering in planetary atmospheres, *Space Science Review, 16*, 527-610.

Hartmann, D.L., M.E. Ockert-Bell, and M.L. Michelsen (1992), The Effect of Cloud Type on Earth's Energy Balance: Global Analysis, J. Climate, 5, 1381-1304.

Hoff, R. M., S. P. Palm, J. A. Engel-Cox, and J. Spinhirne (2005), GLAS long-range transport observation of the 2003 California forest fire plumes to the northeastern US, *Geophys. Res. Lett.*, *32*, L22S08, doi:10.1029/2005GL023723.

Ignatov, A., P. Minnis, N. Loeb, B. Wielicki, W. Miller, S. Sun-Mack, D. Tanre, L. Remer, I. Laslo, and E. Geier (2005), Two MODIS aerosol products over ocean on Terra and Aqua CERES SSF datasets, *J. Atmos. Sci.*, 62(4), 1008-1031, doi:10.1175/JAS3383.1.

Kaufman, Y.J., D. Tanre, L.A. Remer, D. Tanre, E.F. Vermote, A. Chu, and B.N. Holben (1997), Operational remote sensing of tropospheric aerosol over land from EOS moderate resolution imaging spetroradiometer, *J. Geophy. Res.*, **102**, 17,051-17,067.

Kaufman, Y.J., L.A. Remer, D. Tanre, R.R. Li, R. Kleidman, S. Mattoo, R. Levy, T. Eck, B.N. Holben, C. Ichoku, J. Martins, and I. Koren (2005), A critical examination of the residual cloud contamination and diurnal sampling effects on MODIS estimates of aerosol over ocean. *IEEE Trans. Geosci. Remote Sens.*, **43**, 2886-2897.

Kaufman, Y.J., and I. Koren (2006), Smoke and pollution aerosol effect on cloud cover, *Science*, **313**, 655-658.

Kassianov, E.I., and M. Ovtchinnikov (2006), On reflectance ratios and aerosol optical depth retrieval in the presence of cumulus clouds, *Geophy. Res. Lett*, **35**, L06311, doi:10.1029/2007GL032921.

Kobayashi, H., H. Fukushima, T. Murayama, Y. Hagihara, S. Ohta (2003), Optical properties of Asian dust aerosol by SeaWiFS and contemporaneous ground observation data.

Koren, I., L. A. Remer, Y. J. Kaufman, Y. Rudich, and J. V. Martins (2007), On the twilight zone between clouds and aerosols. *Geophys. Res. Lett.*, **34**, L08805, doi:10.1029/2007GL029253.

Marshak, A., and A.B. Davis (2005), Horizontal Fluxes and Radiative Smoothing. In: Marshak, A., and A.B. Davis, [Eds], "*Three-Dimensional Radiative Transfer in Cloudy Atmospheres*", Springer, pp. 543-586.

Marshak, A., G. Wen, J.A. Coakley, L.A. Remer, N.G. Loeb, and R. F. Cahalan (2008), A simple model of the cloud adjacency effect and its impact on retrieved aerosol properties in the vicinity of clouds. *J. Geophys. Res.,* **113**, D14S17, doi:10.1029/2007JD009196.

Moody, E. G., M. D. King, S. Platnick (2005), C. B. Schaaf, and F. Gao, Spatially complete global spectral surface albedos: Value-Added datasets derived from Terra MODIS land products. *IEEE Trans. Geosci. Remote Sens.*, **43**, 144-158.

Nikolaeva O. V., L.P. Bass, T.A. Germogenova, A.A. Kokhanovisky, V.S. Kuznetsov, B. Mayer (2005), The influence of neighboring clouds on the clear sky reflectance with the 3-D transport code RADUGA. *J. Quant. Spectros. Radiat. Transfer.*, **94**, 405-424.

Platnick, S., and S. Twomey (1994), Determining the susceptibility of cloud albedo to changes in droplet concentration with the advanced very high resolution radiometer. *J. Appl. Meteor.*, **33**, 334-347.

Platnick, S. (2000), Vertical photon transport in cloud remote sensing problems. *J. Geophys. Res.*, **105** (D18), 22919-22935.

Platnick, S., M. King, S. Ackerman, W. P. Menzel, B. Baum, J. C. Riedi, and R. A. Frey (2003), The MODIS cloud products: algorithms and examples from Terra, *IEEE Trans. Geosci. Remote Sensing*, vol 41, 459-473.

Reid, J., P. V. Hobbs, R. J. Ferek, D. R. Blake, J. V. Martins, M. R. Dunlap, and C. Liousse (1998), Physical, chemical, and optical properties of regional hazes dominated by smoke in Brazil, *J. Geophys. Res.*, 103, 32,059-32,080.

Remer, L., Y. J. Kaufman, B. N. Holben, A. M. Thompson, and D. McNamara (1998), Biomass burning aerosol size distribution and modeled optical properties, *J. Geophys. Res.*, 103, 31,879-31,891.

Remer, L., and co-authors (2005), The MODIS Aerosol Algorithm, Products, and Validation, *J. Atmos. Sci. Speccial Section*, vol 62, 947-973.

Stephens, G., (1994), Remote Sensing of the Lower Atmosphere: An Introduction, Oxford University Press, pp523.

Tanre, D., Y.J Kaufman, M. Herman, and S. Mattoo (1997), Remote sensing of aerosol properties over oceans using the MODIS/EOS

spectral radiances, *J. Geophy. Res.*, 102, 16,971-16,988.

Thomas, G. E., and K. Stamnes (1999), Radiative Transfer in the Atmosphere and Ocean, Cambridge University Press, pp. 517.

Yamaguchi, Y., A. B. Kahle, H. Tsu, T. Kawakami, and M. Pniel (1998), Overview of Advanced Spaceborne Thermal Emission and Reflection Radiometer (ASTER), *IEEE Trans. Geosci. Remote Sensing*, vol 36, 1062-1071.

Wen, G., R. F. Cahalan, S-C Tsay, and L. Oreopoulos (2001), Impact of cumulus cloud spacingon Landsat atmospheric correction and aerosol retrieval, *J. Geophys. Res.*, 106, 12,129-12,138.

Wen, G., A. Marshak, and R. F. Cahalan (2006), Impact of 3D clouds on clear sky reflectance and aerosol retrieval in a biomass burning region of Brazil, *IEEE Geo. Rom. Sens. Lett.*, 3, 169-172.

Wen, G., A. Marshak, R. F. Cahalan, L. Remer, and R. Kleidman (2007), 3D aerosol-cloud radiative interaction observed in collocated MODIS and ASTER images of cumulus cloud fields, *J. Geophys. Res.*, 112, D13204, doi:10.1029/2006JD008267.

Yang, Y. and L. Di Girolamo (2008), Impact of 3-D radiative effects on satellite cloud detection and their consequences on cloud fraction and aerosol optical depth retrievals, *J. Geophys. Res.*, 113, D04213, doi:10.1029/2007JD009095.

Zhang, J., J. S. Reid, and B. N. Holben (2005), An analysis of potential cloud artifacts in MODIS over ocean aerosol optical thickness products, *Geophys. Res. Lett.,* 32, L15803, doi:10.1029/2005GL023254.